Take it personal! Genetic differences in G protein-coupled receptors as studied with label-free technology

Hillger, J.M.

CHAPTER 3

Whole-cell biosensor for label-free detection of GPCR-mediated drug responses in personal cell lines

Julia M. Hillger

Jeffison Schoop

Dorret I. Boomsma

P. Eline Slagboom

Adriaan P. IJzerman

Laura H. Heitman

Biosens Bioelectron, 2015. **74**: p. 233-242
DOI: https://doi.org/10.1016/j.bios.2015.06.031

Abstract

Deciphering how genetic variation in drug targets such as G protein-coupled receptors (GPCRs) affects drug response is essential for precision medicine. GPCR signaling is traditionally investigated in artificial cell lines which do not provide sufficient physiological context. Patient-derived cell lines such as lymphoblastoid cell lines (LCLs) could represent the ideal cellular model system. Here we describe a novel label-free, whole-cell biosensor method for characterizing GPCR-mediated drug responses in LCLs. Generally, such biosensor technology is deemed only compatible with adherent cell lines. We optimized and applied the methodology to study cellular adhesion properties as well as GPCR drug responses in LCLs, which are suspension cells. Coating the detector surface with the extracellular matrix protein fibronectin resulted in cell adherence and allowed detection of cellular responses. A prototypical GPCR present on these cells, i.e. the cannabinoid receptor 2 (CB_2R), was selected for pharmacological characterization. Receptor activation with the agonist JWH133, blockade by antagonist AM630 as well as downstream signaling inhibition by PTX could be monitored sensitively and receptor-specifically. Potencies and effects were comparable between LCLs of two genetically unrelated individuals, providing the proof-of-principle that this biosensor technology can be applied to LCLs, despite their suspension cell nature, in order to serve as an in vitro model system for the evaluation of individual genetic influences on GPCR-mediated drug responses.

Introduction

Inter-individual variability in drug action and clinical effectiveness forms a challenge in today's drug treatment and development. In fact, variation in drug response that arises from genetic, lifestyle and environmental differences causes even blockbuster drugs to work in only 75% to merely 35% of all [1, 2]. Personalized medicine, or, more broadly defined, precision medicine proposes to personalize drug prescriptions using a sub-population or patient's individual characteristics, e.g. genetic information, and thereby decrease risks of ineffective treatment, dosing or side-effects [2-4]. In order to achieve this, it is paramount to determine whether, and how, genetic variation affects drug responses. Today, genetic testing is available for around 2000 clinical conditions, particularly in oncology [3, 5]. Two poster children of personalized medicine are HER2-positive breast cancer tests as a predictor of response to the drug herceptin and screens for CYP450 polymorphisms that are known to affect treatment with e.g. selective serotonin-reuptake inhibitors [3, 4].

The majority of therapeutic targets to date are formed by a class of membrane proteins, the G protein-coupled receptors (GPCRs) [6]. More than 30% of all currently marketed drugs exert their therapeutic effect by directly binding to and influencing GPCR function. Due to their ubiquity GPCRs are involved in a plethora of physiological processes. It is therefore highly interesting to decipher the influence of genetic variation in GPCR-mediated drug responses [7, 8]. While several examples have linked GPCR polymorphisms to disease and drug response variation, research has mostly focused on the statistics of genotype influences followed by functional characterization in heterologous cell lines [8-10]. Heterologous cell lines are, however, systems with artificial receptor expression and represent a non-physiological, cellular context [11, 12]. To fully understand the underlying mechanism of polymorphism influence, functional characterization on a physiologically relevant molecular and cellular level is vital. An ideal setup would be to use patient-derived cell lines as a model system to assess polymorphism influences on drug response.

A well-established example of such personal cell lines are lymphoblastoid cell lines (LCLs), which to date are a preferred choice for storing a person's genetic material [13, 14]. Numerous consortia have built and actively utilize LCL libraries, including the Centre d'Étude du Polymorphisme Humain (CEPH), the International HapMap and 1000 genomes projects [15-19]. However, LCLs are mainly used as a source of DNA or RNA for genotyping, expression or methylation studies [9, 13]. Functional cellular assays on LCLs have seldom been performed [13, 20, 21] with virtually none for GPCRs. Only Morag and Gurwitz et al. studied the influence of a few GPCR antagonists on LCL growth [20]. In fact, many traditional cellular

assays, especially for GPCRs, are incompatible with LCLs as they require labeling and cell or target engineering. Another drawback is that they generally lack the sensitivity required for such endogenous cell lines which often have low target expression levels. Recently developed label-free technologies offer a more sensitive, less invasive solution and can monitor drug effects on a whole cell in real-time [12, 22, 23]. The sensitivities of these label-free assays is high enough for standard applications such as GPCR activation or inhibition down to detection of small changes such as biased signaling [12, 24]. It may very well be that receptor polymorphisms induce subtle yet important changes in drug-target binding, signaling bias and receptor subtype selectivity [7]. Label-free technologies are therefore ideal for precision medicine purposes, as they harbor the ability to pick up small changes in GPCR signaling or drug responses in the physiologically relevant context of endogenous cells. One disadvantage, however, is that the detection method of label-free assays generally requires cells to adhere to the detector surface at the bottom of the well [12, 23] and unfortunately, LCLs are by nature non-adherent suspension cells [25]. However, several reports have been published recently on the application of label-free technology to suspension cells, including various types of blood cells [26, 27]. To solve the above listed challenges we developed a methodology for a label-free, impedance-based whole-cell assay that allows characterization of GPCR signaling in LCLs despite their suspension cell nature. This enables the use of LCLs as an in vitro cellular model system to evaluate individual differences in GPCR-mediated drug responses.

Material and methods

Chemicals and reagents

The LCLs were kindly provided within the framework of this collaboration [15]. Fibronectin from bovine plasma, poly-D-lysine (PDL) and unsupplemented RPMI 1640 cell culture medium were purchased from Sigma Aldrich (Steinheim, Germany). Collagen I from rat tail was purchased from Fisher Scientific (Illkirch, France). The GPCR agonist JWH133 was purchased from TOCRIS (Bristol, UK), ATP from Sigma Aldrich and AM630 from Cayman Chemicals Company (Ann Arbor, Michigan, USA). RGD peptide (GRGDTP) and RGE peptide (GRGESP) were purchased from AnaSpec/Tebu-bio (Heerhugowaard, the Netherlands). $G\alpha_i$ blocking pertussis toxin (PTX) was purchased from Sigma Aldrich. All other chemicals were of analytical grade and obtained from standard commercial sources.

Lymphoblastoid cell line generation

The LCLs had previously been generated at the Rutgers Institute (Department of Genetics, Piscataway, NJ, USA) using a standard transformation protocol [15]. In short, peripheral B-lymphocytes were exposed to Epstein–Barr Virus (EBV) by treatment with filtered medium from a Marmoset cell line in the presence of phytohemaglutinin (PHA) during the first week of culture [13, 14, 28]. Cultures were maintained for 8–12 weeks to adapt and expand the EBV transformed lymphocytes and subsequently cryopreserved.

Cell culture

Two LCLs from two genetically unrelated individuals were used for the experiments presented in this manuscript. Cryopreserved cells were thawed, resuscitated and multiple aliquots frozen for future use. Of note, LCLs were disposed of after culturing them for maximally 120 days. LCLs were grown as suspension cells in culture medium consisting of RPMI 1640 (25 mM HEPES and $NaHCO_3$) supplemented with 15% Fetal Calf Serum (FCS), 50 mg/mL streptomycin and 50 IU/mL penicillin at 37 °C and 5% CO_2. Cells were subcultured twice a week at a ratio of 1:5 on 10 cm ø plates.

Label-free whole-cell biosensor analysis (xCELLigence RTCA system)

Detection principle

Whole-cell assays were performed using the xCELLigence RTCA system [12], a real-time cell analyzer (RTCA) based on the electrical impedance generated by cells attaching to gold electrodes embedded on the bottom of the microelectronic E-plates. Cell attachment changes the local ionic environment at the electrode-solution interface, thereby generating impedance. Such relative changes in impedance (*Z*) are summarized as a dimensionless parameter, the so-called Cell Index (CI), and displayed in a real-time plot. In detail, a very weak electrical signal is applied to the sensor electrodes, where the AC excitation voltage level is in the lower mV range and the resulting current is in the µA range (output test signal is 22 mV rms ± 20% with max. 5 mV DC offset at 10, 25 and 50 kHz). The RTCA analyzer determines cell indeces at these three predetermined optimal midrange frequencies and the average speed of measurement is approximately 150–250 ms for each individual well. In order to increase usability and ease for the user, the RTCA system provided by the manufacturer has pre-set conditions for amplitude, applied potential, frequency range and used frequency for extrapolation of results [29, 30], which were used in all experiments

presented in this manuscript. The CI value at a given time point is defined by the formula in **Eq. (1)**:

Equation (1) $CI = (Z_i - Z_0)\ \Omega / 15\ \Omega$

where Z_i is the impedance at each individual time point and Z_0 represents the baseline impedance in the absence of cells, which is measured prior to the start of the experiment. The CI in the absence of cells is therefore defined as 0. As cells adhere to the electrodes, impedance and the corresponding CI increase proportionally. Impedance changes thereby reflect variations in cell number and degree of adhesion, as well as cellular viability and morphology [12, 22]. Such cellular parameters are also affected upon activation of GPCR signaling, thereby resulting in impedance changes and real-time monitoring of cellular signaling events [12]. Typically, GPCR-mediated activation would result in an increase in cell adhesion and overall increase in CI, while a lower CI would indicate loss of adhesion [31].

General protocol

The wells of 16 or 96 well E-plates were coated with 50 µl of fibronectin (10 µg/ml), unless stated otherwise. After 30 min incubation at room temperature, the coating liquid was removed and all plates were air dried for at least 1 h prior to use. LCLs were harvested by re-suspending in cell culture medium after brief treatment with EDTA and centrifuged twice at 200*g* for 5 min. Background impedance (Z_0) was measured after adding 45 µL, or in case of antagonist experiments 40 µL, of culture media to 16 or 96 well E-plates, respectively. In all cases, final well volumes after cell and ligand addition were 100 µL. Cells were seeded by adding 50 µL of cell suspension containing 50,000 cells per well, unless stated otherwise. To ensure accurate seeding densities, cells were counted using Trypan blue staining and a BioRad TC10 automated cell counter. After resting at room temperature for 30–60 min, the E-plate was placed into the recording station situated in a 37 °C and 5% CO_2 incubator. Impedance was measured every 15 min overnight. Cells were stimulated by a GPCR ligand or vehicle control in 5 µl after 18–20 h, unless specified otherwise. To record GPCR activation, CI was recorded for at least 30 min with a recording schedule of 15 s intervals for 20 min, followed by intervals of 1 min, 5 min and finally 15 min.

For assay optimization purposes, cells were stimulated with the purinergic P2Y receptor agonist ATP at a saturating concentration of 100 µM. As compound solubility of JWH133 and AM630 required addition of dimethylsulfoxide (DMSO), the final DMSO concentration upon ligand or vehicle addition was kept at 0.25% DMSO for all wells and assays. For agonist assays,

cells were stimulated with increasing concentrations of JWH133. For antagonist assays, cells were pre-incubated for 30 min with 5 µl of the antagonist AM630 at increasing concentrations or vehicle control. Subsequently, cells were challenged with a submaximal agonist concentration equal to the agonist's EC_{80} value (100 nM for JWH133) or vehicle control.

For coating trials, wells were coated with 50 µl of varying coatings such as poly-D-lysine (0.1 mg/ml), collagen I (50 µg/ml), pure Fetal Calf Serum or fibronectin (0.1–50 µg/ml). Non-coated wells were used as control condition. After removing coating liquid, only poly-D-lysine plates were washed with 3×100 µl PBS before use.

To assess the specificity of LCL adherence to fibronectin, assay medium was supplemented with increasing concentrations of the integrin blocking RGD peptide GRGDTP [1 µM–1 mM] or the inactive control RGE peptide GRGESP [1 mM]. Normal assay medium was used as control and non-coated wells were used for reference.

For studies on $G\alpha_i$ coupling, cells were seeded in assay medium containing 100 ng/ml Pertussis Toxin (PTX).

Data analysis

Experimental data were obtained with RTCA Software 1.2 (Roche Applied Science) and subsequently exported and analyzed using GraphPad Prism 5.0 (GraphPad Software Inc., San Diego, CA, USA). For data analysis, ligand responses were normalized to Δ cell index (Δ CI) after subtracting baseline (vehicle control) to correct for any agonist-independent effects. Overall, a threshold of 0.01 Δ CI was kept for considering responses different from baseline. Peak responses were defined as highest Δ CI observed within 30 min after compound addition. Peak values and experimental Δ CI traces were exported to Prism for further analysis; construction of bar graphs or dose-response curves by nonlinear regression and calculation of IC_{50}, EC_{50} and EC_{80} values. All values obtained are means of at least three independent experiments performed in duplicate. Statistical significance was determined using Student's *t*-test for two values or two column comparison, e.g. comparing pEC_{50} values between individuals. Comparison of the means of multiple data sets, e.g. the peak Δ CI of ATP responses of various coating conditions, was performed by one-way ANOVA, followed by a Tukey's post test for comparison of all columns or a Dunnett's post test when comparing to vehicle or non-coated control. To get an indication of statistical assay reproducibility under optimized assay conditions, correlation analysis was performed for the dose–response curves for both the CB_2R agonist as well as antagonist for each cell line.

Results

Coating allows detection of GPCR responses

At first various common coatings known to mediate cellular adherence were tested for their ability to allow detection of GPCR signaling in LCLs, for which ATP was chosen as a typical GPCR ligand. The result of a representative coating experiment is shown in **Fig. 1**. Following LCL seeding, an initial increase in impedance related to cell adhesion, growth and division was observed (**Fig. 1A**). The overall levels of impedance after 1 h and 18 h, i.e. shortly prior to ligand addition, are summarized in **Fig. 1B** and **C**. Impedance levels after 1 h are likely to reflect initial cellular adhesion, while impedance after 18 h is also influenced by cellular proliferation or more prolonged changes in cellular morphology. Subsequent addition of the agonist ATP induced changes in LCL morphology that were recorded in real-time (**Fig. 1A** and **D**). Typically, ATP addition resulted in an immediate dose-dependent increase of impedance to a peak level. Subsequently, the CI trace gradually decreased towards a plateau within a period of 30 min.

Lack of coating resulted in no adherence or detection of GPCR response. Even though poly-D-lysine initially caused a high amount of cellular adherence equal to fibronectin (**Fig. 1B**) this declined drastically over the course of 18 h (**Fig. 1C**) and allowed little to no detection of GPCR response (**Fig. 1D** and **E**). Even though both poly-D-lysine and collagen coating resulted in significant impedance levels in comparison to non-coated wells just before ATP addition (18 h, **Fig. 1C**), both of them failed to allow detection of an ATP-induced response (**Fig. 1D** and **E**) as growth curves had dropped to or below baseline levels (CI<0). Fibronectin coating, on the other hand, did mediate cellular adherence over a longer time course resulting in a stable growth curve and sufficient window for detection of GPCR signaling (**Fig. 1D** and **E**).

Of note, coating experiments performed on LCLs from a second individual, individual 2, gave virtually identical results (*data not shown*).

Subsequently, the amount of fibronectin required for stable impedance levels and GPCR signal detection was further optimized. While initially all amounts of fibronectin resulted in impedance above non-coated levels (**Fig. 2A** and **B**), only fibronectin levels from 5 µg/ml or higher maintained impedance above non-coated up to 18 h (**Fig. 2A** and **C**). Significant ATP signaling was detected from 10 to 50 µg/ml fibronectin coating (**Fig. 2D** and **E**). In fact, 25 and 50 µg/ml were indistinguishable in impedance level and ATP response window. 10 µg/ml resulted in slightly lower effects, but still gave stable impedance levels and response window,

which were both not statistically significantly different from 25 or 50 µg/ml. Fibronectin concentration effects were comparable for another cell line from individual 2 (*data not shown*). Therefore, a fibronectin concentration of 10 µg/ml was chosen for all further experiments.

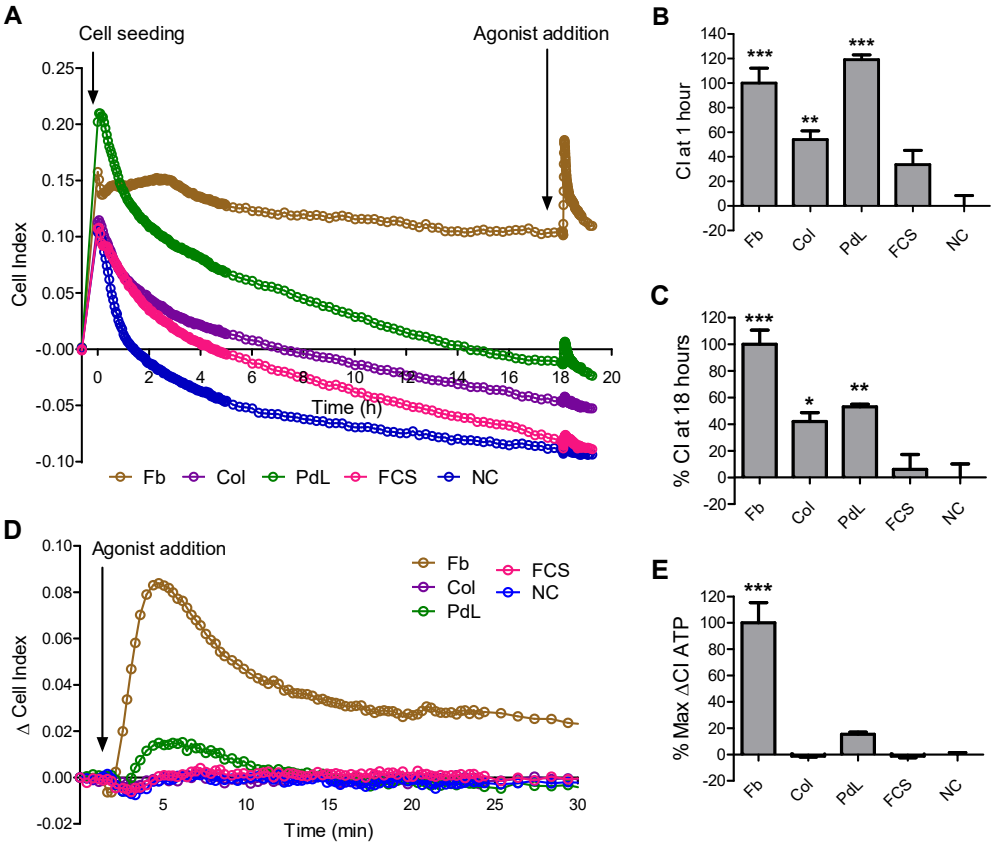

Figure 1. Fibronectin coating mediates LCL adhesion to allow detection of GPCR response. Electrodes were coated with various standard coatings, i.e. fibronectin (Fb; [50 µg/ml]), collagen I (Col; [50 µg/ml]) poly-D-lysine (PdL; [0.1 mg/ml]) and Fetal Calf Serum (FCS). Non-coated (NC) wells were used as a control. Cells were stimulated with the agonist (ATP [100 µM]) after 18 h of growth. Representative xCELLigence traces of a full experiment (**A**) and a baseline-corrected ATP response (**D**) are given. Time point 0 represents the time of cell seeding (**A**) and agonist addition (**D**), respectively. Bar graphs summarize the differences in cell index (CI) shortly after seeding (**B**, 1 h) and prior to agonist addition (**C**, 18 h), both normalized to fibronectin (100%) and non-coated (0%) wells. (**E**) Bar graph of baseline-corrected Δ cell index (Δ CI) of peak ATP response per coating condition, normalized to fibronectin (100%) and non-coated (0%) wells. Data are mean ± SEM from three separate experiments performed in quadruplicate (**B, C**) and duplicate (**E**) using one cell line (individual 1, 50,000 cells/well). Significance compared to control was tested using one-way ANOVA with Dunnett's post-hoc test. *=p<0.05, **=p<0.01, ***=p<0.001.

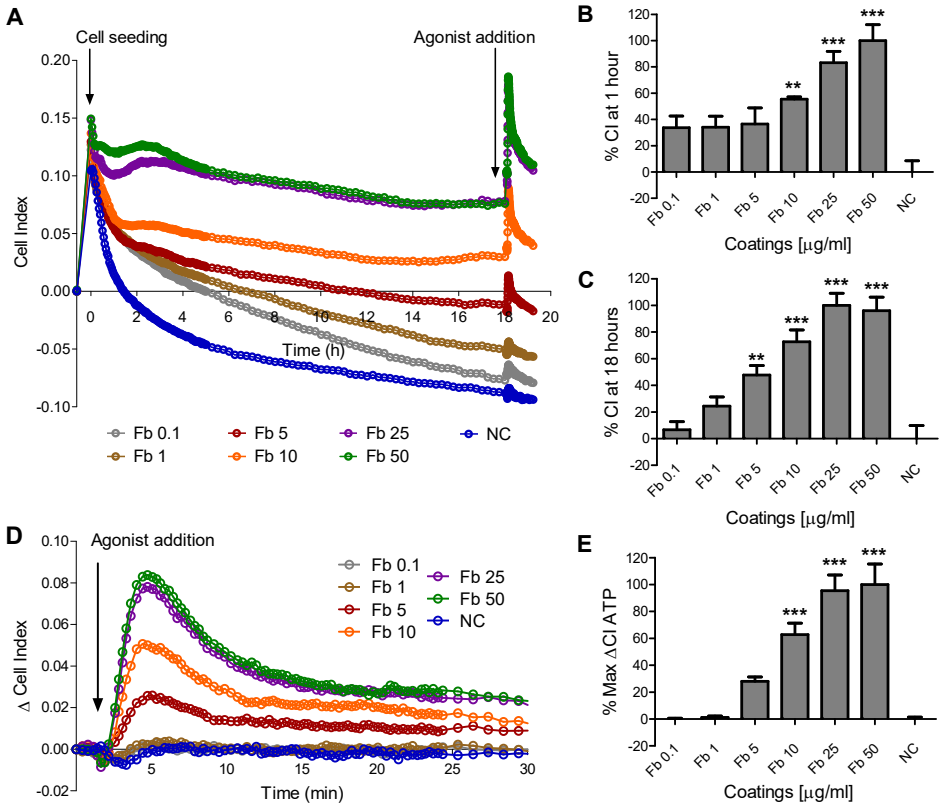

Figure 2. Titration of fibronectin coating concentration. Electrodes were coated with different amounts of fibronectin from 0.1–50 µg/ml. Non-coated (NC) wells were used as a control. Cells were stimulated with agonist (ATP [100 µM]) 18 h after seeding. Representative xCELLigence traces of a full experiment (**A**) and a baseline-corrected GPCR agonist response (**D**) are given. Time point 0 represents time of cell seeding (**A**) or agonist addition (**D**). Bar graphs indicate the cell index (CI) shortly after seeding (B, 1 h) and prior to agonist addition (C, 18 h), both normalized to fibronectin (100%) and non-coated (0%) wells. (**E**) Bar graphs represent the baseline-corrected Δ cell index (Δ CI) at peak ATP response, normalized to fibronectin (100%) and non-coated (0%) wells. Data are mean ± SEM from three separate experiments performed in quadruplicate (**B, C**) and duplicate (**E**) using one cell line (individual 1, 50,000 cells/well). Significance compared to control was tested using one-way ANOVA with Dunnett's post-hoc test. *=p<0.05, **=p<0.01, ***=p<0.001.

LCLs specifically adhere to fibronectin

In order to confirm the specificity of LCLs' interaction with fibronectin, inhibition of fibronectin adherence by small, integrin-targeting peptides containing the RGD motif was characterized. Addition of RGD peptide to the assay medium decreased the LCLs' attachment to fibronectin, as reflected by a decreased cell index (**Fig. 3A** and **B**), though not to levels as low as the non-coated control. This inhibition was concentration-dependent (**Fig. 3B**). However the effect decreased over time and was not noticeable after 18 h or, therefore, on

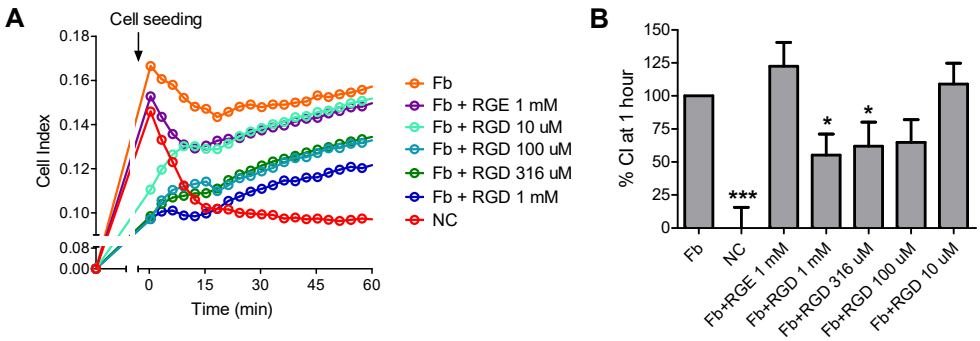

Figure 3. Influence of peptides blocking the fibronectin interaction. Cells were seeded on fibronectin coated plates (Fb; [10 µg/ml]) in assay medium containing varying concentrations of RGD peptide [1 mM–1 µM], inactive reference peptide RGE [1 mM] or normal medium. Non-coated (NC) wells were used as reference. Cells were stimulated by agonist addition (ATP [100 µM]) after 18 h growth. (**A**) Representative full xCELLigence traces, where time point 0 represents the time of cell seeding. (**B**) Bar graphs indicate cell index (CI) 1 h after seeding, normalized to fibronectin (100%) and non-coated (0%) wells. Data derived from six separate experiments performed in quadruplicate using LCLs of one individual (individual 1, 50,000 cells/well). Statistical significance versus control RGE peptide was determined using one-way ANOVA with Dunnett's post-hoc test. *=p<0.05, **=p<0.01, ***=p<0.001.

ATP response *(data not shown)*. Treatment with the inactive RGE peptide at a high concentration (1 mM) did not affect any part of the impedance readout, thereby confirming that LCL adherence was affected by specific inhibition of integrin–fibronectin interactions. Similar experiments performed on LCLs from a second individual, individual 2, gave comparable results (*data not shown*).

Seeding density and stimulation time affect GPCR response

Next to optimization of coating, assay conditions were further optimized by evaluating various LCL densities. The experimental results are summarized in **Fig. 4**. Both the height of the growth curves (**Fig. 4A** and **B**) and the GPCR signal (**Fig. 4C** and **D**) increased accordingly with the cell density.

The cell index after 18 h (**Fig. 4B**) was significantly different between all seeding densities, except between 50,000 and 25,000 cells/well. While 25,000 and 50,000 cells/well showed no statistically significant difference in growth curve, they did show significant differences in detection of an ATP signal (**Fig. 4D**). 25,000 cells/well gave an insufficient window for full pharmacological characterization and was not statistically different from the control. 50,000 Cells/well, however, was sufficient to allow a reliable detection of a GPCR signal. Interestingly, the ATP response was not statistically different from the condition with

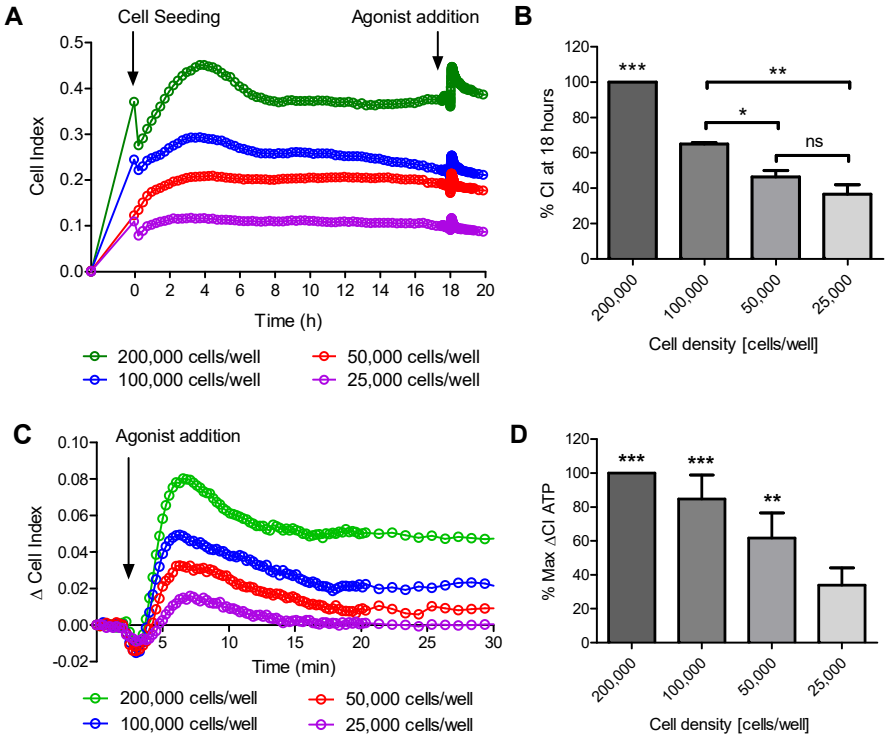

Figure 4. Seeding density influences growth curve and window of GPCR response. Cells were seeded in four different densities (25,000–200,000 cells/well). Cells were stimulated with the agonist (ATP [100 µM]) after 18 h of growth. Representative xCELLigence trace of a full experiment (**A**) and a baseline-corrected ATP response (**C**). Time point 0 represents the time of cell seeding (**A**) or agonist addition (**C**). Bar graphs indicate the cell index (CI) shortly prior to agonist addition normalized to CI=0 (**B**, 18 h) and baseline-corrected Δ cell index (Δ CI) at peak ATP response, normalized to vehicle control (**D**). Data are mean ± SEM from three separate experiments performed in quadruplicate (**B**) and duplicate (**D**) using one cell line (individual 1). Statistical significance was determined using one-way ANOVA with Tukey post-hoc test to compare all columns to each other (**B**) and Dunnett's post-hoc test to compare values to vehicle control (**D**). ns=not significant (p>0.05), *=p<0.05, **=p<0.01, ***=p<0.001.

100,000 cells/well. Irrespective of specific statistical significances, both the basal level of impedance as reflected in the growth curve and the ATP response increase in height along with the seeding density. As 50,000 cells/well was the lowest cell density that allowed reliable measurements of GPCR activation, this cell density was chosen for all further experiments. Similar experiments performed on LCLs from a second individual, individual 2, gave comparable results (*data not shown*).

Additionally, as the LCL's growth curve appeared to reach a stable plateau much earlier than 18–20 h (**Fig. 5A**), stimulation after 5 h was also investigated. GPCR stimulation after

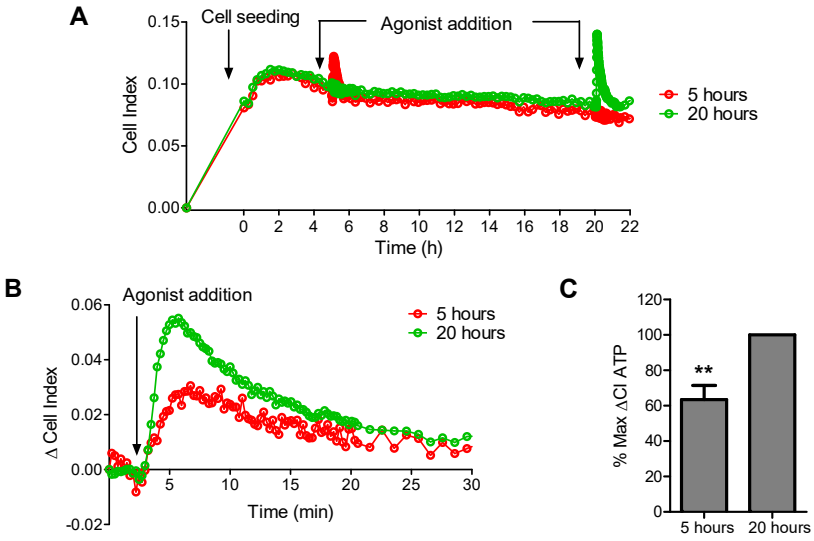

Figure 5. Influence of growth phase duration. Two cell lines were stimulated with the GPCR agonist ATP [100 µM] immediately after reaching growth plateau at 5 h or after a longer duration of growth at 20 h. Representative xCELLigence traces of a full experiment (**A**) and a baseline-corrected ATP response (**B**). Time point 0 represents the time of cell seeding (**A**) or agonist addition (**B**). (**C**) Bar graphs indicate the baseline-corrected Δ cell index (Δ CI) at peak ATP response, normalized to vehicle control. Data represents means of four separate experiments performed in duplicate using the LCLs of one individual (individual 1, 50,000 cells/well). Statistical significance was determined using Student's *t*-test. *=p<0.05, **=p<0.01, ***=p<0.001.

20 h gave a significantly higher response than stimulation after 5 h, despite the fact that the growth curve plateau had been reached after 5 h (**Fig. 5B** and **C**). Comparable effects were observed on LCLs from a second individual (*individual 2, data not shown*).

Detailed pharmacological characterization of GPCR signaling in LCLs is possible

After completing assay optimization, the resulting protocol was applied for full pharmacological characterization of an example GPCR. For this purpose, a GPCR with well characterized pharmacology and known to be expressed in LCLs was chosen, i.e. the cannabinoid receptor 2 (CB_2R; Ensembl gene: ENSG00000188822). A result of a representative experiment along with concentration-effect curves is provided in **Fig. 6**. Responses from two cell lines from two unrelated individuals were recorded and compared.

Addition of a CB_2R selective agonist JWH133 resulted in an immediate and concentration- dependent increase of impedance (**Fig. 6A** and **B**), which was similar in shape to the recorded ATP responses (**Fig. 1**, **Fig. 2** and **Fig. 3**). The impedance increase was concentration-dependently reduced by pretreatment with the CB_2R selective antagonist

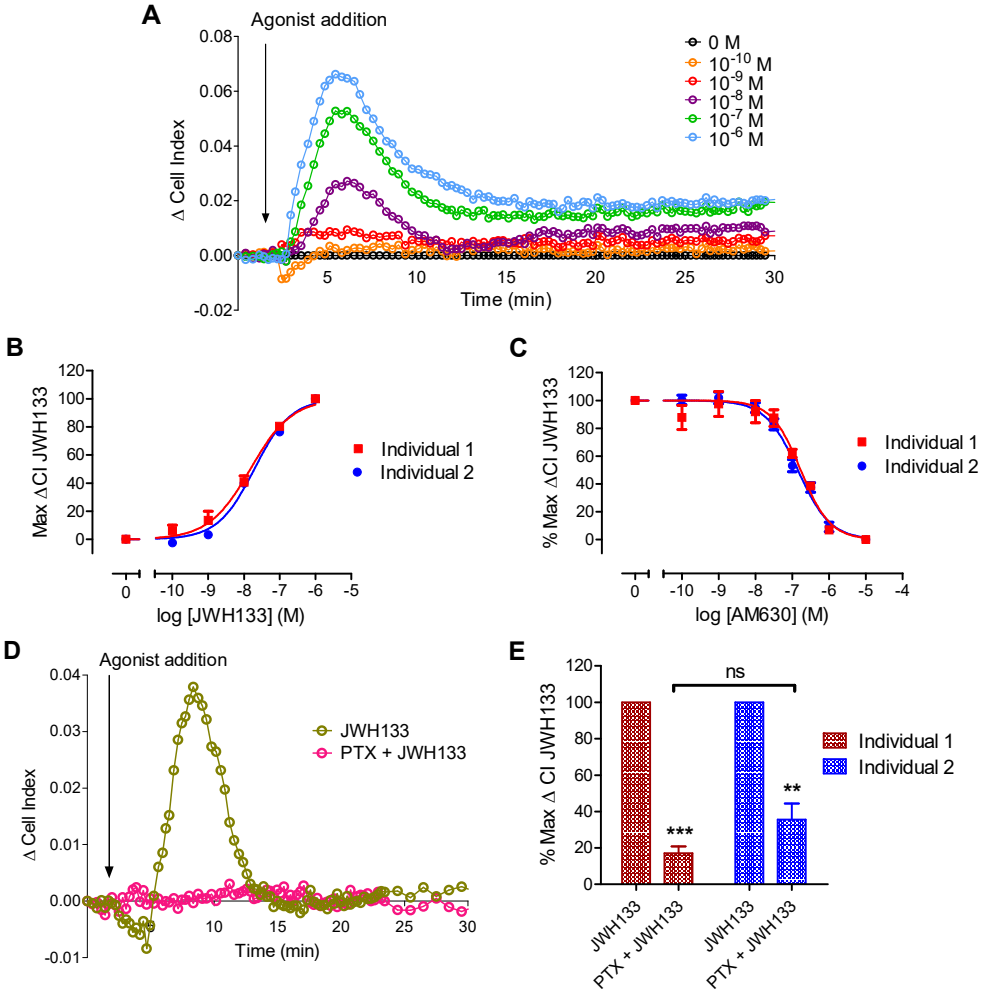

Figure 6. Characterization of Cannabinoid receptor 2 responses in two genetically unrelated LCLs. Cell lines were stimulated with a CB_2R selective agonist JWH133 18 h after seeding (50,000 cells/well). (**A**) Representative example of a baseline-corrected JWH133 response [1 µM–100 pM]. (**B**) Dose-response curves of JWH133 derived from peak Δ cell index (Δ CI) within 30 min after agonist addition. pEC_{50} values of JWH133 were 7.82±0.07 (individual 1) and 7.71±0.04 (individual 2). (**C**) Cell lines were pre-incubated for 30 min with increasing concentrations of AM630 [10 µM–100 pM] before stimulation with JWH133 [EC_{80}: 100 nM]. Dose-response curves of AM630 were derived from peak Δ CI within 30 min after agonist addition. pIC_{50}values for AM630 were 6.77±0.06 (individual 1) and 6.85±0.04 (individual 2). To test coupling to $G\alpha_i$proteins, cells were seeded and grown in assay medium with or without PTX [100 ng/ml] and stimulated with JWH133 [EC_{80}: 100 nM]. (**D**) Representative example of baseline-corrected JWH133 response in the absence and presence of PTX. (**E**) Bar graphs show the PTX effect on peak Δ cell index (Δ CI) of JWH133 response, normalized to vehicle control. Data represents the means of four separate experiments performed in duplicate. Statistical significance was calculated by Student's *t*-test. ns=not significant ($p>0.05$), *=$p<0.05$, **=$p<0.01$, ***=$p<0.001$. pEC_{50} and pIC_{50} values did not differ significantly between the two individuals.

AM630 (**Fig. 6C**). Concentration-effect curves were obtained by peak analysis of corresponding agonist-induced CI changes. Potencies of JWH133, given as pEC_{50} values, were 7.82±0.07 (15 nM) and 7.71±0.04 (20 nM) on individual 1 and individual 2, respectively. Antagonist IC_{50} values for AM630 were obtained by stimulating cells with a submaximal (EC_{80}) concentration of JWH133 following antagonist pre-incubation. The pIC_{50} values for AM630 were 6.77±0.06 (169 nM) and 6.85±0.04 (141 nM) on individual 1 and individual 2, respectively. Both agonist pEC_{50} and antagonist pIC_{50} values did not differ significantly between the two individuals. In order to get an indication of overall assay reproducibility under these optimized conditions, correlation analysis was performed for the dose–response curves for both the CB_2R agonist as well as antagonist. Experiments were reproducible with a coefficient of correlation (Pearson's r) of minimum 0.95 (p<0.05) for both individuals and at all concentrations of the agonist and 0.85 for the antagonist (p<0.01).

The influence of blocking the $G\alpha_i$-coupled pathway upon CB_2R activation was examined for both cell lines, as shown in **Fig. 6D** and **E**. Addition of PTX to the assay medium effectively diminished the CB_2R response to agonist JWH133 (**Fig. 6D**) in a similar manner for both cell lines (**Fig. 6E**). This confirmed that the LCLs' response to the selective CB_2R agonist was dependent on the $G\alpha_i$ pathway.

Discussion

Personal cell lines, such as LCLs that are commonly used for storing an individual's genetic material [13], can offer a model system to investigate individual differences in drug response in a physiologically relevant, cellular context. The introduction of highly sensitive, label-free technologies that allow cellular assays with minimal modifications makes harvesting this potential possible. In the present study, we have setup and optimized a label-free methodology for investigating GPCR-mediated drug responses in LCLs and characterized a prototypical GPCR for proof-of-principle.

As P2Y receptors (Ensembl family: ENSFM00760001715026) are abundantly present on virtually all cell types, including LCLs [32, 33], ATP was chosen as initial ligand for the methodological setup. In fact, P2Y receptors represent one of the few examples with functional characterization in LCLs. Lee et al. investigated ATP-induced P2Y receptor responses in LCLs using a single-cell fluorescent microscopy technique. While this traditional, label-based technique measured little response at an ATP concentration of 100 µM, the label-free assay used in our study was able to measure a clear response at the same concentration (**Fig. 1**, **Fig. 2**,**Fig. 3**, **Fig. 4** and **Fig. 5**). This emphasizes the advantage and

opportunity of using label-free techniques to measure GPCR signaling in LCLs over traditional, label-based methodologies, as they offer highly increased sensitivity and lower detection limits.

The initial experimental setup was based on previously published protocols for adherent cell lines [24, 31, 34]. While label-free assays are often deemed incompatible with suspension cells, some application examples exist for various label-free assays based on optical or impedance detection. These include various types of blood cells. For instance, GPCR signaling was measured in primary human neutrophils and THP-1 cells, a human monocyte cell line, using an optics-based assay [27, 35]. The impedance-based CellKey technology was used to measure GPCR signaling in monocyte cell lines (THP-1 and U937), neutrophils and primary normal peripheral blood monocytes (PBMCs) [36, 37]. Both these technologies have the disadvantage of being performed in buffer and at room temperature, while xCELLigence assays use more physiologically relevant conditions like normal cell culture medium and a temperature of 37 ˚C. Application of xCELLigence technology to suspension cells has been reported, however not for investigating GPCR signaling. Obr *et al*. [38] applied the technology to measure the effect of histone deacetylase inhibitors on hematopoietic cells. Martinez-Serra *et al.* [26] investigated the cytotoxic effect of antineoplastic agents on cells from hematological malignancies, which included the leukemia lymphoblast cell line K562. It is well known that the cell density and distribution on the electrodes can significantly influence impedance and experimental readout [12, 22, 23]. In previous cases, fibronectin was often used to achieve cell adherence combined with increased cell densities with an optimal range of 60,000 to 45,000 cells/well [26, 27, 35, 38]. Accordingly, we first tested various standard coating conditions and optimized cell density for impedance recordings in LCLs and found similar conditions to be optimal for LCLs. In our hands, LCL densities of 50,000 cells/well were sufficient for detection of a robust GPCR response (**Fig. 4**), a number that is merely 2.5-fold higher than common for adherent cells [24, 31, 34] and very comparable to existing suspension cell protocols described above.

Following LCL seeding onto fibronectin-coated plates, an initial increase in impedance related to cell adhesion, growth and division was observed, as is similar for any adherent cell line [31, 34]. Fibronectin was capable of mediating LCL adherence sufficiently for the measurement of a GPCR response after 18 h (**Fig. 1**) in a concentration-dependent manner (**Fig. 2**). It has been shown that LCLs can attach to fibronectin [39] and that LCLs express the α4β1 and αvβ3 type integrins [40], which are known to interact with fibronectin [41, 42]. Most fibronectin-binding integrins interact with a RGD tripeptide active site of fibronectin [41-43]. Small soluble RGD peptides have been shown to compete for integrin binding [43,

44] and one of those partially blocked the LCL's cellular interaction with the fibronectin coating (**Fig. 3**). The inactivity of the RGE control peptide confirmed that adherence was due to a specific interaction of LCL's integrins with fibronectin. Interestingly, around 50% of LCL adherence remained even in the presence of a high concentration of the RGD peptide. This remaining adhesion is most likely mediated through another motif in fibronectin, the LDV motif, which is known to be the predominant binding site for the α4β1 integrin [42]. Poly-D-lysine is known to mediate cellular adhesion by changing surface charges [45, 46], but failed to maintain LCL adherence at sufficiently high levels for detection of an ATP response despite an initially equally high adherence as fibronectin (**Fig. 1**). LCLs have been shown to attach to poly-L-lysine at the same concentration, however, for a shorter timeframe than the 18 h in our experiments, i.e. 4 h [33]. Moreover, collagen, which also mediates cellular adhesion through specific integrins [41], failed to promote adhesion of LCLs. Collagen-interacting integrins are thus likely not present in LCLs, while fibronectin-specific integrins are. Furthermore, the findings agree with Martinez-Serra *et al*. who showed that cells from hematological malignancies, including the leukemia lymphoblast cell line K562, attached more efficiently to fibronectin than to collagen, laminin or gelatin [26].

Following the methodological optimization, we showed that in-depth pharmacological characterization of GPCRs is possible in LCLs using the CB_2 receptor as a prototypical example (**Fig. 6**). This receptor is well expressed in LCLs [47] and has been investigated in a heterologous cell line on the xCELLigence [31], but has not yet been functionally characterized in LCLs until now. With recombinant cell lines, it is straightforward to confirm that an impedance signal is receptor-specific by using the untransfected parental cell line as negative control [31, 34]. However, this is not possible for endogenously expressed receptors, as is the case for LCLs used in this study. Therefore, proof of a receptor-specific response was provided by the concentration-dependent receptor activation with a CB_2 receptor selective agonist, JWH133, and inhibition of that response by a CB_2 receptor selective antagonist, AM630 [31, 48, 49]. Both JWH133 and AM630 effects were comparable between LCLs from two different individuals (**Fig. 6**), as was expected as both cell lines carried the same genotype for all non-synonymous variants (*data not shown*). Furthermore, both JWH133 and AM630 effects on LCLs were comparable to literature values obtained in heterologous cell lines. Scandroglio et al. determined the potency of JWH133 and AM630 in traditional and label-free assays using a for GPCR investigations typical heterologous cell system, a recombinant CHO cell line. Agonist JWH133 had a comparable potency in both impedance and traditional cAMP assays of 29.9±20.5 nM and 30±7.3 nM, respectively, showing that label-free assays yield values equal to traditional techniques. Similarly,

JWH133's potency determined in the present study on LCLs (pEC_{50}: 7.82±0.07 (15 nM) for individual 1, 7.71±0.04 (20 nM) for individual 2) were very comparable to Scandroglio et al.'s values on the CHO-cells. Furthermore, these authors showed that AM630 was able to antagonize JWH133's effects, however they did not report an IC_{50} value for this inhibition. Literature values for AM630 include an IC_{50} of 128.6±40.6 nM in a traditional cAMP assay on a recombinant CHO cell line [48]. On LCLs, AM630 readily antagonized JWH133 effects with a very comparable potency (pIC_{50}: 6.77±0.06 (169 nM) for individual 1, 6.85±0.04 (141 nM) for individual 2).

Besides for measuring cellular effects on GPCR signaling by agonists or antagonists, the label-free xCELLigence system is also well suited to monitor inhibition of downstream pathways [31, 50]. The CB_2 receptor is known to predominantly couple to the $G\alpha_i$-pathway and it was previously shown that JWH133 signaling on CHO cells could be inhibited by $G\alpha_i$-blocker PTX [31, 51]. Similarly, PTX effectively diminished the CB_2R response to JWH133 in LCLs of both individuals (**Fig. 6**), which thereby confirmed that the LCLs' response to the agonist was indeed dependent on the Gαi-pathway. Taken together, the effects of JWH133 in LCLs are mediated by the CB_2 receptor. While the effects and potencies of the CB_2R ligands were comparable between the endogenous LCLs and the recombinant CHO cells, LCLs represent a more relevant physiological context as they are cell lines with specific individual genetic material.

LCLs already form a large resource for personalized medicine research, as they are commonly used to investigate association of genetic variation to disease or drug response [9, 13, 21]. Moreover, large libraries of LCLs have already been built and are actively utilized in numerous consortia [15-19]. Investigation of GPCR drug responses in LCLs may further help the advancement of precision medicine. Examples linking GPCR polymorphisms to drug response to date are sparse and focus on statistic associations followed by validating polymorphism influences by generating these variants in heterologous cell lines [10]. Heterologous cell lines, however, are labor intensive to make and represent a different, non-physiological cellular context than cells of an individual [11, 12]. Receptor overexpression, differences in intracellular metabolic conditions as well as products from other genes could modify cellular responses. Therefore, screening receptor responses in LCLs from persons with potentially interesting polymorphisms may offer a more direct way of validation. Expression studies indicate that LCLs express a wide range of druggable GPCRs that are of interest for drug research, besides the CB_2 and P2Y receptors investigated in this study [47]. Next to investigation of GPCRs, label-free technology offers a wide range of other

applications and has similarly been applied to other important classes of drug targets, such as receptor tyrosine kinases [52, 53].

Conclusion

In conclusion, the current paper shows that direct characterization of GPCR activity in LCLs is possible with a highly sensitive label-free technology, the xCELLigence. Despite that such biosensor technology is deemed only compatible with adherent cell lines, we were able to optimize the assay for the suspension cell LCLs. Using the CB_2R as a prototypical GPCR, we were able to show that receptor activation by an agonist, blockade by an antagonist, as well as inhibition of downstream signaling could be monitored sensitively and receptor-specifically. The resemblance of cellular responses between LCLs from two unrelated individuals confirms that the methodology is robust and applicable to LCLs in general. This offers the ability to use LCLs not just as a mere source of DNA for genetic studies, but also as a functional, physiologically more relevant cellular model system for detailed investigation of GPCR pharmacology in vitro. Ultimately, a mechanistic link may be made between polymorphisms and drug response variation in individuals. Thus combining the resolution power of a whole-cell label-free method with LCLs opens vast possibilities for research on precision medicine.

Acknowledgments

This research was supported by the Center for Collaborative Genomic Studies on Mental Disorders at the National Institute of Mental Health (NIMH) [NIMH U24 MH068457-06]. The LCLs used in this study were kindly provided within the framework of this collaboration [15] and are part of the Netherlands Twin Registry (NTR; *http://www.tweelingenregister.org/en/*), part of the Center for Collaborative Genomic Studies on Mental Disorders [NIMH U24 MH068457-06]. Data and biomaterials (such as cell lines) are available to qualified investigators and may be accessed by following a set of instructions stipulated on the NIMH website (*https://www.nimhgenetics.org/access_data_biomaterial.php*).

We thank Dr. A. Brooks (Department of Genetics, Rutgers University, Piscataway, NJ, USA) for preparation of the lymphoblastoid cell lines and Prof. E.A.J.M. Goulmy (Transplantation biology, Leiden University and Leiden University Medical Center, Leiden, the Netherlands) for her advice on the research and manuscript.

References

1. Carey, J. *Making personalized medicine pay*. BusinessWeek 2010 [cited 2015 24.06.2015]; Available from: *http://www.bloomberg.com/bw/magazine/content/10_05/b4165058407403.htm*.
2. van't Veer, L.J. and R. Bernards, *Enabling personalized cancer medicine through analysis of gene-expression patterns.* Nature, 2008. **452**(7187): p. 564-70.
3. Mirnezami, R., J. Nicholson, and A. Darzi, *Preparing for precision medicine.* The New England journal of medicine, 2012. **366**(6): p. 489-91.
4. Katsanis, S.H., G. Javitt, and K. Hudson, *Public health. A case study of personalized medicine.* Science, 2008. **320**(5872): p. 53-4.
5. Weng, L., et al., *Pharmacogenetics and pharmacogenomics: a bridge to individualized cancer therapy.* Pharmacogenomics, 2013. **14**(3): p. 315-24.
6. Overington, J.P., B. Al-Lazikani, and A.L. Hopkins, *How many drug targets are there?* Nat Rev Drug Discov, 2006. **5**(12): p. 993-6.
7. Venkatakrishnan, A.J., et al., *Molecular signatures of G-protein-coupled receptors.* Nature, 2013. **494**(7436): p. 185-94.
8. Sadee, W., et al., *Genetic variations in human G protein-coupled receptors: implications for drug therapy.* AAPS pharmSci, 2001. **3**(3): p. 54-80.
9. Docherty, S.J., et al., *A genetic association study of DNA methylation levels in the DRD4 gene region finds associations with nearby SNPs.* Behav Brain Funct, 2012. **8**: p. 31-44.
10. Ishiguro, H., et al., *Brain cannabinoid CB2 receptor in schizophrenia.* Biol Psychiatry, 2010. **67**(10): p. 974-82.
11. Eglen, R. and T. Reisine, *Primary cells and stem cells in drug discovery: emerging tools for high-throughput screening.* Assay Drug Dev Technol, 2011. **9**(2): p. 108-24.
12. Yu, N., et al., *Real-time monitoring of morphological changes in living cells by electronic cell sensor arrays: an approach to study G protein-coupled receptors.* Anal Chem, 2006. **78**(1): p. 35-43.
13. Sie, L., S. Loong, and E.K. Tan, *Utility of lymphoblastoid cell lines.* J Neurosci Res, 2009. **87**(9): p. 1953-9.
14. Sugimoto, M., et al., *Steps involved in immortalization and tumorigenesis in human B-lymphoblastoid cell lines transformed by Epstein-Barr virus.* Cancer research, 2004. **64**(10): p. 3361-4.
15. Willemsen, G., et al., *The Netherlands Twin Register biobank: a resource for genetic epidemiological studies.* Twin Res Hum Genet, 2010. **13**(3): p. 231-45.
16. Abecasis, G.R., et al., *A map of human genome variation from population-scale sequencing.* Nature, 2010. **467**(7319): p. 1061-73.
17. Welsh, M., et al., *Pharmacogenomic discovery using cell-based models.* Pharmacological reviews, 2009. **61**(4): p. 413-29.
18. Dausset, J., et al., *Centre d'etude du polymorphisme humain (CEPH): collaborative genetic mapping of the human genome.* Genomics, 1990. **6**(3): p. 575-7.
19. Wheeler, H.E. and M.E. Dolan, *Lymphoblastoid cell lines in pharmacogenomic discovery and clinical translation.* Pharmacogenomics, 2012. **13**(1): p. 55-70.

20. Morag, A., et al., *Human lymphoblastoid cell line panels: novel tools for assessing shared drug pathways.* Pharmacogenomics, 2010. **11**(3): p. 327-40.
21. Li, L., et al., *Discovery of genetic biomarkers contributing to variation in drug response of cytidine analogues using human lymphoblastoid cell lines.* BMC genomics, 2014. **15**: p. 93-115.
22. Fang, Y., *Label-Free Receptor Assays.* Drug Discov Today Technol, 2011. **7**(1): p. e5-e11.
23. Rocheville, M., et al., *Mining the potential of label-free biosensors for seven-transmembrane receptor drug discovery.* Progress in molecular biology and translational science, 2013. **115**: p. 123-42.
24. Stallaert, W., et al., *Impedance responses reveal beta(2)-adrenergic receptor signaling pluridimensionality and allow classification of ligands with distinct signaling profiles.* PLoS One, 2012. **7**(1): p. e29420.
25. Avila-Carino, J., et al., *Search for the critical characteristics of phenotypically different B cell lines, Burkitt lymphoma cells and lymphoblastoid cell lines, which determine differences in their functional interaction with allogeneic lymphocytes.* Cancer Immunol Immunother, 1991. **34**(2): p. 128-32.
26. Martinez-Serra, J., et al., *xCELLigence system for real-time label-free monitoring of growth and viability of cell lines from hematological malignancies.* OncoTargets and therapy, 2014. **7**: p. 985-94.
27. Schroder, R., et al., *Applying label-free dynamic mass redistribution technology to frame signaling of G protein-coupled receptors noninvasively in living cells.* Nat Protoc, 2011. **6**(11): p. 1748-60.
28. Miller, G. and M. Lipman, *Release of infectious Epstein-Barr virus by transformed marmoset leukocytes.* Proceedings of the National Academy of Sciences of the United States of America, 1973. **70**(1): p. 190-4.
29. *RTCA DP Instrument Operator's Manual, version 2013.* ACEA Biosciences Inc.
30. *RTCA SP Instrument Operator's Manual, version 2013.* ACEA Biosciences Inc.
31. Scandroglio, P., et al., *Evaluation of cannabinoid receptor 2 and metabotropic glutamate receptor 1 functional responses using a cell impedance-based technology.* Journal of biomolecular screening, 2010. **15**(10): p. 1238-47.
32. Jacob, F., et al., *Purinergic signaling in inflammatory cells: P2 receptor expression, functional effects, and modulation of inflammatory responses.* Purinergic signalling, 2013. **9**(3): p. 285-306.
33. Lee, D.H., et al., *Expression of P2 receptors in human B cells and Epstein-Barr virus-transformed lymphoblastoid cell lines.* BMC immunology, 2006. **7**: p. 22-33.
34. Guo, D., et al., *Functional efficacy of adenosine A(2)A receptor agonists is positively correlated to their receptor residence time.* British journal of pharmacology, 2012. **166**(6): p. 1846-59.
35. Gedge, L., *Corning® Epic® Label-Free Cell-Based Assay: Development of a Suspension Cell Assay Using a Human Monocyte Cell Line (THP-1 Cells).* Corning Life Sciences Application note, 2010.
36. Leung, G., et al., *Cellular Dielectric Spectroscopy: A Label-Free Technology for Drug Discovery.* Journal of the Association for Laboratory Automation, 2005. **10**(4): p. 258-269.

37. Molecular Devices Inc., *Analyzing Endogenous Receptors in Non-Adherent Cell Lines and Primary Cells with the CellKey Small Sample 96W Microplate.* CellKey System Application Highlight 5, 2008.
38. Obr, A., et al., *Real-time monitoring of hematopoietic cell interaction with fibronectin fragment: the effect of histone deacetylase inhibitors.* Cell adhesion & migration, 2013. **7**(3): p. 275-82.
39. Stupack, D.G., et al., *Matrix valency regulates integrin-mediated lymphoid adhesion via Syk kinase.* The Journal of cell biology, 1999. **144**(4): p. 777-88.
40. Rincon, J., J. Prieto, and M. Patarroyo, *Expression of integrins and other adhesion molecules in Epstein-Barr virus-transformed B lymphoblastoid cells and Burkitt's lymphoma cells.* International journal of cancer. Journal international du cancer, 1992. **51**(3): p. 452-8.
41. Humphries, J.D., A. Byron, and M.J. Humphries, *Integrin ligands at a glance.* Journal of cell science, 2006. **119**(Pt 19): p. 3901-3.
42. Johansson, S., et al., *Fibronectin-integrin interactions.* Frontiers in bioscience : a journal and virtual library, 1997. **2**: p. d126-46.
43. Gilchrist, C.L., et al., *Functional integrin subunits regulating cell-matrix interactions in the intervertebral disc.* Journal of orthopaedic research : official publication of the Orthopaedic Research Society, 2007. **25**(6): p. 829-40.
44. Atienza, J.M., et al., *Dynamic monitoring of cell adhesion and spreading on microelectronic sensor arrays.* Journal of biomolecular screening, 2005. **10**(8): p. 795-805.
45. Jacobson, B.S. and D. Branton, *Plasma membrane: rapid isolation and exposure of the cytoplasmic surface by use of positively charged beads.* Science, 1977. **195**(4275): p. 302-4.
46. Yavin, E. and Z. Yavin, *Attachment and culture of dissociated cells from rat embryo cerebral hemispheres on polylysine-coated surface.* The Journal of cell biology, 1974. **62**(2): p. 540-6.
47. Vincent, M., et al., *Genome-wide transcriptomic variations of human lymphoblastoid cell lines: insights from pairwise gene-expression correlations.* Pharmacogenomics, 2012. **13**(16): p. 1893-904.
48. Ross, R.A., et al., *Agonist-inverse agonist characterization at CB1 and CB2 cannabinoid receptors of L759633, L759656, and AM630.* British journal of pharmacology, 1999. **126**(3): p. 665-72.
49. Howlett, A.C., et al., *International Union of Pharmacology. XXVII. Classification of cannabinoid receptors.* Pharmacological reviews, 2002. **54**(2): p. 161-202.
50. Schroder, R., et al., *Deconvolution of complex G protein-coupled receptor signaling in live cells using dynamic mass redistribution measurements.* Nature biotechnology, 2010. **28**(9): p. 943-9.
51. Gkoumassi, E., et al., *Virodhamine and CP55,940 modulate cAMP production and IL-8 release in human bronchial epithelial cells.* British journal of pharmacology, 2007. **151**(7): p. 1041-8.
52. Atienza, J.M., et al., *Label-free and real-time cell-based kinase assay for screening selective and potent receptor tyrosine kinase inhibitors using microelectronic sensor array.* Journal of biomolecular screening, 2006. **11**(6): p. 634-43.
53. Zhuang, G., et al., *Phosphoproteomic analysis implicates the mTORC2-FoxO1 axis in VEGF signaling and feedback activation of receptor tyrosine kinases.* Science signaling, 2013. **6**(271): p. ra25.